Annals of the Academy of Romanian Scientists
Series on Physics and Chemistry
Online ISSN 2559-1061 Volume **4**, Number **1**/**2019**

A REVIEW OF AERONET SUN-PHOTOMETER MEASUREMENTS OF THE AEROSOL PROPERTIES AT SITE EFORIE NORD ROMANIA

Sabina ȘTEFAN[1]

Abstract. *Due to their effects, the aerosols have a profound impact on air quality and affect the earth's energy budget. As a result, the interest in studying aerosol properties increased in recent decades. It is known that the scattering and absorbing radiation processes act directly on the radiative budget of atmosphere-earth system. However, estimating their magnitude requires increased effort to improve measurements and datasets from regional to global scales. This study focuses on knowledge concerning the photometry technique to determine the physical properties of aerosols and to assess the aerosol characteristics of tropospheric aerosols using solar photometry data from the Romanian Eforie Nord AERONET station. The aerosol optical properties are assesses by focusing on the sun-photometer CIMEL CE-318 measurements for two time periods 2010-2012 and 2015-2017. The results emphasize that the area on the Black Sea coast is characterized by a good air quality, and that the meteorological conditions had influenced the measurements much more during the second period.*

Keywords: solar photometry, sun-photometer, AERONET, aerosol optical properties

1. Introduction

Atmospheric aerosol plays an important role by interacting with radiation and modifying cloud microphysical properties. Thus, aerosol particles participate in Earth's energy budget both *directly,* by scattering and absorbing radiation [1, 2], and *indirectly* by acting as cloud condensation nuclei and, thereby, by affecting cloud properties [3, 4, 5]. Also, aerosol particles in the atmospheric boundary layer influence air quality and can be damaging to human health [6,7,8]. Therefore, it is very important to monitor the aerosols concentration and their properties, in order to gather data from as many parts of the globe as possible and from across various time spans. Different ground-based and satellite instruments are used to study the aerosol properties and dynamics on the regional and global scales. Special national, regional and global networks were created in order to study aerosols in specific regions of the world and on a global scale. A global network, the AErosol Robotic NETwork (AERONET) is formed from many sun-photometer international networks https://aeronet.gsfc.nasa.gov/, [9]. In Romania, there is also a national sun-photometer network associated to the Romanian Atmospheric Observatory (RADO).

[1] University of Bucharest, Faculty of Physics, 077125 Magurele, Ilfov, Romania, Academy of Romanian Scientists, Splaiul Independenței 54, Bucharest, Romania.

The typical values of the columnar aerosol optical depth (AOD), Ångström exponent (AE), particle single-scattering albedo (SSA), refractive index (RI), and size distribution were determined using measurements from the six AERONET sites [10-15].

AERONET measurements performed at 6 sites in different locations throughout Romania during the 2007-2017 period have revealed the different trends of the fine and coarse modes AOD and AE, dependent upon geographical and meteorological conditions [13].

This study aims to review the results of the aerosol characteristics for two periods 2010-2012 and 2015-2017 from the measurements provided by the sun-photometer #397. Section 2 of this article briefly discusses the atmospheric aerosol properties (2.1) and the solar photometry technique used in aerosol measurements in AErosol RObotic NETwork (AERONET) (2.2). Section 3 examines findings on aerosol optical depth, Ångström exponent values, single-scattering albedo and turbidity from the Eforie Nord station in the AERONET network. The last section provides the study's conclusions.

2. Solar Photometry in characterizing tropospheric aerosols

2.1. About atmospheric aerosol

Atmospheric aerosol is defined as a polydisperse system containing liquid and solid particles suspended in atmospheric air except hydrometers. Aerosol particles come from natural sources and anthropogenic sources.

2.1.1. General considerations

According to the formation mode, the aerosol is of two kinds: primary and secondary. Primary aerosol comes from natural sources, and is created through the dispersion of earth-borne materials caused by wind, volcanic emissions, or evaporation from water surfaces and / or anthropogenic sources. Primary aerosol may consist of soil, carbon, clay, mineral, ash, carbon black or marine salt particles [16].

Secondary aerosol is the result of chemical reactions and condensation/conversion of gases and vapors in the atmosphere. The anthropic aerosol has different sources, intermediate substances produced in various phases of the technological processes. Estimation of global anthropogenic aerosol emissions is based on the knowledge of aerosol production consumptions and activities and the emission factors calculated for these processes.

Through its direct and indirect effects, atmospheric aerosol influences the Earth's energy balance. The direct effect of the atmospheric aerosol is the result of the

scattering and absorption of solar radiation, while the indirect effect is due to its fundamental role in the microphysics of the clouds. Through its indirect effect, the aerosol changes the size and density of cloud droplets. The latter modify the albedo, the cloud's lifetime and the amount of precipitation [17-20]. Small cloud droplets are less efficient in producing precipitation than large droplets. Furthermore, a large number of aerosol particles lead to a longer cloud life time. The indirect effect sometimes results in a low rate of surface evaporation, a more stable and dry atmosphere, and consequently a reduction in cloud formation [21].

Emissions due to human activity can be estimated. However, the aerosol transported from a distance is important but very difficult to quantify.

2.1.2. Microphysical properties of atmospheric aerosol

In general, the two essential physical parameters of the atmospheric aerosol are the mass or numerical concentration and the dimensional distribution of aerosols. The evolution of remote measurement techniques (remote sensing) of the atmospheric composition has made it possible to obtain concentration profiles with a very high accuracy.

The variation in the mass concentration (μ/m ^{3}) and numerical concentration (#/m^3) depends on local sources of natural or anthropic aerosol, but also on its remote transport. In essence, the dimensional distribution of the aerosol is a statistic of the aerosols in the atmosphere according to the size (diameter) thereof.

Depending on the studied process, the statistics of these particles are calculated by number, by total area, or by the volume of aerosol in the atmosphere. Thus, when considering, for example, cloud formation processes or processes occurring in living organisms following inhalation of aerosols, the number of particles, *N(r*), in volume units (the concentration numerical) which have the radius between *r* and (*r* + *dr*)is used.

When studying the catalysis processes of gaseous reactions occurring on the surface of aerosol particles, or when considering aerosol effects on health, the aerosol free surface statistic is the most important element. That is, the area of the total free surface, *S(r),* of the particles in the volume unit having the radius between r and *(r + dr):*

$$S = S_1 + S_2 + S_3 \; cu \; S_i = \pi D_{gi}^2 N_i \exp\left(2 \ln^2 \sigma_{gi}\right) \quad (1)$$

The preferred unit of measure for *S (r)* is μm^2/cm^3.

When studying the effects of aerosol attenuation of solar radiation, but also in certain health-related issues of subjects inhaling aerosol, it is very important to know the volumetric aerosol statistics. That is, the volume *V(r)* of the particles in the volume unit having the radius between *r* and (*r* + *dr*):

$$V = V_1 + V_2 + V_3 \; cu \; V_i = \frac{\pi}{6} D_{gi}^3 N_i \exp\left(\frac{9}{2}\ln^2 \sigma_{gi}\right) \tag{2}$$

The unit of measure for $V(r)$ is $\mu m^3/cm^3$.

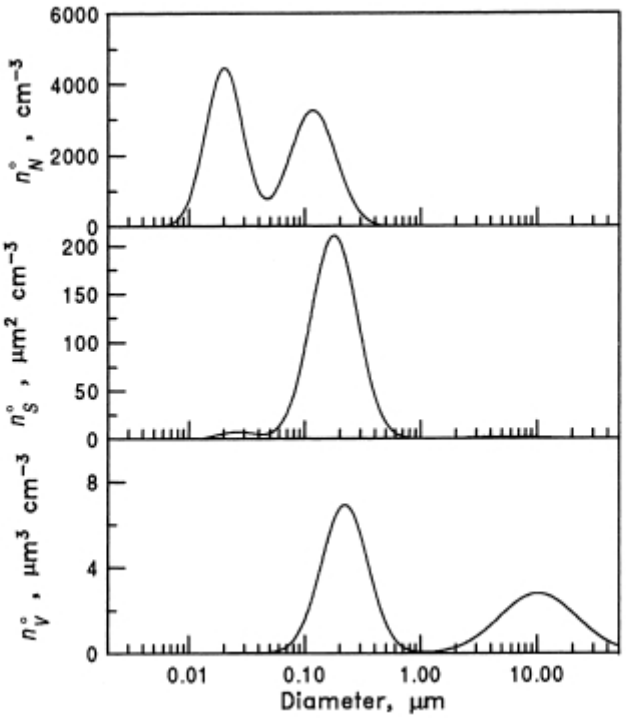

Fig. 1. Modes of numerical, surface and volume distribution of aerosol particles (Seinfeld and Pandis, 1998, [22]).

Direct experimental determinations on the aerosol have demonstrated that, regardless of the statistics in which they are represented, the particle distribution in the atmosphere extends over several orders of magnitude of the diameters and reaches some maximal values at certain dimensions. This means that the aerosol particles can be grouped into several preferential sizes, called modes (Figure 1). Aerosol modes have specific names.

Thus, particles with several nanometer diameters form the *ultrafin (or nucleation) mode*. Particles with diameters between 10 nm and 0.1 μm, which occur mainly through gaseous condensation, form the Aitken mode. The group of diameters between 0.1μm and 1 m is called the *accumulation mode.* The latter are generally produced by the anthropogenic sources. Finally, the particles with diameters larger than 1μm, predominantly of natural origin, are considered to form the *coarse mode* [23].

It should be noted that it is not necessary to provide so many details of the structure of the aerosol in the practical calculations of light extinction. For example, the aerosol volume distribution from the urban atmosphere (which carries the greatest interest in the anthropic action) has only two significant maximal values. In this sense, the particles from the nucleation mode, the Aitken particles, and the accumulation mode form a single distinct way, called *fine mode* [24, 25, 26].

As a result, the dimensional distribution has a bimodal character. The expressions of distribution functions were generally deduced by using different methods for measurements. For instance, Fitzgerald (1978) [27] uses the 4-parameter Gamma function as the distribution function, which rightfully captures dimensional spectra of the atmospheric aerosol:

$$n(r) = Ar^{\alpha} \exp(-Br^{\gamma}) \tag{3}$$

where A, B, α, γ are positive parameters.

The logarithmic type is another form of the frequently-used dimensional distribution function, and it represents the sum of three logarithmic distributions [22]:

$$\frac{dn}{d\log D_p} D_p = \sum_{i=1}^{3} \frac{N_i}{\sqrt{2\pi}\ln \sigma_g} \exp\left[-\frac{(\ln D_p - \ln D_{gi})^2}{2\ln^2 \sigma_{gi}}\right] \tag{4}$$

With N_i the number of aerosol particles, expressed in cm^{-3}; σ_{gi} - the geometric standard deviation; D_{gi} - geometric diameter, in μm.

The statistical parameters mean radius, modal, effective radius, and total volume concentrations for fines and coarse aerosol particles can all be calculated for a given type of distribution function [22]:

$$\ln r_m = \frac{\int_{r_{\min}}^{r_{\max}} \ln r \frac{dN(r)}{d\ln r} d\ln r}{\int_{r_{\min}}^{r_{\max}} \frac{dN(r)}{d\ln r} d\ln r} \tag{5}$$

$$r_{ef} = \frac{\int_0^{\infty} r^3 \frac{dN(r)}{d\ln r} d\ln r}{\int_0^{\infty} r^2 \frac{dN(r)}{d\ln r} d\ln r} = r_m \exp(2{,}5\sigma^2) \tag{6}$$

where σ is the standard deviation (for all modes) average:

$$\sigma = \sqrt{\frac{\int_{r_{\min}}^{r_{\max}} \left(\ln r - \ln r_m\right)^2 \frac{dN(r)}{d\ln r} d\ln r}{\int_{r_{\min}}^{r_{\max}} \frac{dN(r)}{d\ln r} d\ln r}} \tag{7}$$

Total volume, fine and coarse is expressed in $\mu m^3/\mu m^2$:

$$C_V = \int_{r_{min}}^{r_{max}} \frac{dV(r)}{dlnr} d\,lnr = \int_{r_{min}}^{r_{max}} \frac{dV(r)}{dr} dr \tag{8}$$

The separation between fine and coarse modes is provided by the radius value for which the volume dimensional distribution is minimal.

Among the properties of the aerosol, one must not forget the shape of the particles, which in recent years are increasingly being measured to determine the type of aerosols and the sources from which they originate. Knowledge of the chemical composition of the atmospheric aerosol allows us to understand both the direct and indirect radiation effects, which explains the formation of clouds and precipitation.

According to aerosol sources and composition, the aerosol was divided into several types, which were used to determine the aerosol optical parameters. Thus, Mielonen *et al*. (2009) [28] classified aerosol types into coarse absorbing (dust), coarse non-absorbing (marine), mixed absorbing (polluted dust), fine absorbing (biomass burning), and fine non-absorbing (polluted continental) by using the Ångström exponent and single-scattering albedo (SSA) from AERONET data.

2.2. General Considerations on Solar Photometry

The notion of solar photometry is somewhat improper. Instead, solar radiometry would be a more appropriate concept, since the wavelength range investigated through photometry far exceeds the visible field of electromagnetic radiation [29]. However, the term solar photometry has started to be used more and is now commonly referenced in works that tackle specifically the atmospheric composition. The Sun is the source of solar photometry. As the main source of energy for Earth, it is optically regarded as a black radiator at a temperature of 6000K in its center and at about 5000K at the limit of the photosphere. Irradiance Be, B-brightness and Sun's emissivity are attenuated by the Earth's atmosphere and are influenced by the effects of sunspots, sun's altitude, etc.

Direct solar radiation transits the atmosphere, which is a relatively opaque and rather heterogeneous environment, with a very variable refractive index.

The spectral distribution of solar radiation depends on the components of the atmosphere. Generally, atmospheric aerosol produces strong scattering, absorption, and polarization of direct solar radiation. As such, the effects of aerosol in the atmosphere are of interest to both air quality and influence on Earth's radiation balance and consequently on climatic variability.

The theoretical study of light extinction in optical media containing finely suspended particles is produced by using an important simplification hypothesis, namely the simple scatter approximation. This approximation is not valid for cloudy photometric measurements. The scattering and absorption of light on a spherical dielectric object is described by a solution of the Maxwell equations named Mie's generic name, after the name of the German physicist Gustav Mie, who developed it in 1908 [30].

At present, technological development allows for the detection of atmospheric components, and mainly of aerosols, at local and at distance, by remote sensing. Aerosol remote sensing techniques – both locally and carried remotely – could be passive or active techniques. The passive remote sensing techniques use a natural light source, most often the sun, whereas the active ones use their own source, most often a laser. Solar photometry and satellite imagines are passive remote sensing techniques. As the main instruments for passive remote sensing used to measure atmospheric aerosol loading, sun-photometers provide the necessary information on the optical and microphysical properties of the aerosol throughout the atmospheric column. The optical depth (τ or AOD) of the aerosol is the main parameter captured through sun photometers. The AOD is the main optical parameter, the measure of the aerosols (e.g. urban haze, smoke particles, desert dust, sea salt) distributed within a column of air from the instrument (Earth's surface) to the top of the atmosphere [9]. The AOD spectral dependence contains important information about the type and the size of the aerosol found in the atmosphere.

2.2.2. Sun photometer. Aerosol Robotic Network (AERONET)

The AOD is determined by local observations, using sun photometers located on the ground, fixed stations, marine vessels (for the purpose of determining AOD in remote seas) and on aerial platforms (airplanes). The goal is to determine the variation of the AOD, as well as its content of aerosol with altitude. In general, the AOD measurements with a ground-mounted instrument have a limited utility. Studies have shown that it is much more useful to correlate the data obtained from several fixed stations connected to the network and to compare the results to other types of atmospheric measurements (e.g. LIDAR, radiometers, satellite observations, meteorological data, sampling, etc.).

AERONET is by far the best-developed international network. The AERONET Monitoring Network was created by NASA and was expanded in collaboration with many other international research institutions [31]. Another interesting aspect of this network relates to the validation of the measurements obtained through satellite instruments. AERONET consists of a large number of sun photometers [32] which automatically transmit measured data.

This network has already had a service life of over 20 years, during which time it had produced observations of AOD and almost-real-world celestial irradiations, which it distributed globally. Furthermore, the AERONET network is continuously expanding through the co-opting of national laboratories interested in climate and environmental studies globally. In addition to basic products, AERONET *al*so provides derived parameter values, such as particle size distribution of aerosol particles, simple scattering albedo, and complex refractive index. This network was developed to produce aerosol information through two types of measurements obtained on the ground: spectral data of extinction of direct solar radiation (i.e. AOD), and angular distribution of celestial radiance. The CIMEL CE-318 sun photometer is the underlying instrument (Figure 2).

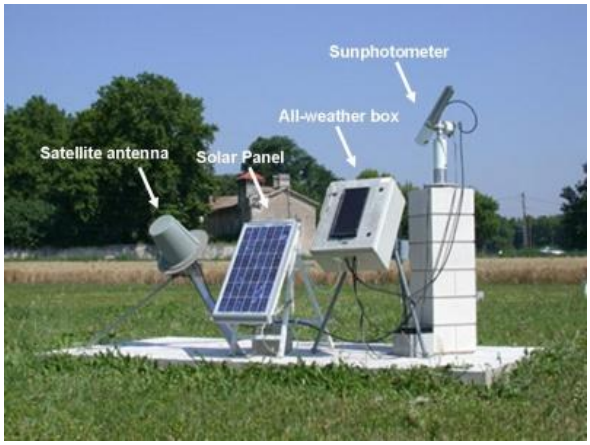

Fig. 2. Sun photometer's components [33] from http://aeronet.gsfc.nasa.gov/index.html).

The CE-318 photometer is composed of a photodetector, optical system, spectral filter, automatic sun tracking system, as well as a data recording and acquisition system. There are two detectors: one for measuring direct sunlight, and one for celestial radiation. The position of the sun is calculated taking into account time, latitude and longitude. The photometer performs measurements of direct radiation in eight spectral bands: 340-1020 nm, 440 nm, 670 nm, 870 nm, 940 nm, 1020 nm. Background radiation measurements are performed for wavelengths of 440 nm, 670 nm, 870 nm and 1020 nm. Measurements are taken at time intervals that are calculated in order to increase the measurement accuracy [9].

The wavelength ranges are chosen in accordance with the absorption of radiation in the atmosphere. Most measuring channels are dedicated to the study of aerosols. The following three categories of information on somewhat independent aerosols can be obtained from solar photometry measurements: 1) Specific Optical Deepness (AOD), which is a measure of the aerosol columnar concentration; 2) mean AOD spectral variation given by the exponent / parameter Ångström (AE or α); 3) the spectral dependence (curvature) of the Ångström parameter (δa). The complex interaction of aerosols with radiation is commonly understood using also the other aerosol optical parameters, such as: the single-scattering albedo (SSA or ω), the complex refractive index, the Ångström parameter and the precipitated water content in the air column determined by observations on the specific channel of 940 nm.

The radiation parameters used in the analysis of the interaction of solar radiation with aerosol through photometry are:

- Phase function, P (Θ; λ), for 83 scattering angle values;

- The asymmetry factor, $\langle \cos\Theta \rangle$, for each value of the phase function;

- Spectral flows at top of the atmosphere (TOA) and bottom of the atmosphere (BOA): downward fluxes, $F_{TOA}^{\downarrow}(\lambda), F_{BOA}^{\downarrow}(\lambda)$ and upward flows, $F_{TOA}^{\uparrow}(\lambda)$, $F_{BOA}^{\uparrow}(\lambda)$.

The spectral flows are calculated in broad band by integration between 0.2 and 4.0 μm. The calculations are based on the values of the real and complex refractive indices obtained through the AERONET typical wavelength inversion algorithm. Interpolations/extrapolations of the spectral dependence of the refractive indices are performed for the purpose of integration.

Radiative forcing (expressed in W/m^2):

$$\Delta F_{TOA} = F_{TOA}^{\uparrow} - F_{TOA}^{\uparrow 0}; \Delta F_{BOA} = F_{BOA}^{\downarrow} - F_{BOA}^{\downarrow 0}$$

Efficiency of radiative forcing (expressed in W/m^2):

$$\Delta F_{TOA}^{eff} = \frac{\Delta F_{TOA}}{\tau(\lambda = 0{,}55\,\mu m)} \text{ and } \Delta F_{BOA}^{eff} = \frac{\Delta F_{BOA}}{\tau(\lambda = 0{,}55\,\mu m)} \quad (9)$$

The methodology for determining the aerosol charge, i.e. the total optical depth τ_{tot} (AOD), from the air column involves a solar photometer in order to calculate the relationship between the measured voltage and the incidence of incident radiation, based on the Beer-Lambert-Boguer law:

$$V(\lambda) = V_0(\lambda) d^2 exp[-\tau(\lambda)_{tot} \cdot m] \quad (10)$$

where V is the digital voltage measured at wavelength λ, V_o is the extraterrestrial voltage, d is the ratio of the average to the actual Earth-Sun distance, and m is the optical air mass [9].

Other atmospheric constituents can scatter light and must be considered when calculating the AOD. The optical depth due to water vapor, Rayleigh scattering, and other wavelength-dependent trace gases must be subtracted from the total optical depth to obtain the aerosol component [9]:

$$\tau(\lambda)_{Aerosol} = \tau(\lambda)_{tot} - \tau(\lambda)_{water} - \tau(\lambda)_{Rayleigh} - \tau(\lambda)_{O3} - \tau(\lambda)_{NO2} - \tau(\lambda)_{CO2} - \tau(\lambda)_{CH4} \quad (11)$$

The standard AERONET networking, instrument maintenance and calibration, cloud surveillance, and data processing allow for a quantitative comparison of the aerosol data at different times and locations. Extracting information from such data is done by using so-called inversion algorithms [34, 35].

Inversion algorithms allow for the indirect aerosol information to be obtained by fitting measurements across the irradiation field at 440, 670, 870 and 1020 nm on a radiation transfer pattern. The radiation field is determined by the complex aerosol refractive index (wavelength dependent) and by the size distribution of the aerosol particles (in the range of 0.05-15μm) across the entire atmospheric column.

It should be noted that the modal distribution of the aerosol is the basic hypothesis of the inversion algorithm. The inversion algorithm is based on a set of model hypotheses. The benchmark of fulfilling these assumptions in practical situations is a measure of the quality of the algorithm results.

And yet, the dimensional distribution of aerosol particles is not the only product of the inversion algorithm.

In combination with solar photometry data (AOD), a number of optical properties of the aerosol can be obtained in the total atmospheric column. Thus, Holben B.N. *et al.*,1998, Eck, T.F.,*et al.*, 1999; B. Schmid *et al.*, 2001, [9,36, 37] were able to determine, through the use of inversion algorithm, precipitable water and Ångström parameter for example, as follows.

The total column *water vapor amount* determination uses three channels: 675nm, 870nm, and 940nm. The total transmission (T) is computed for 675nm and 870nm using Rayleigh and aerosol optical depths. The equation for precipitable water (in cm) is [38]:

$$u = \frac{\left[\frac{-lnT_W}{a}\right]^{1/b}}{m_W} \quad (12)$$

where u is the precipitable water in cm, T_w is the transmission due to water vapor, a and b are filter-dependent constants, and m_w is the water vapor optical air mass.

Angstrom parameter

The size distribution of aerosols can be estimated from spectral aerosol optical depth, typically from 440nm to 870nm. The negative slope (or first derivative) of AOD with wavelength in logarithmic scale is known as the Ångström parameter (Å or α). Values of α greater than 2.0 indicate that fine mode particles exist (e.g. smoke particles and sulfates), whereas values of α near zero indicate the presence of coarse mode particles such as desert dust [36].

$$\alpha(\lambda) = -\frac{d(\ln \tau_\lambda)}{d(\ln \lambda)};\ \alpha = -\frac{\ln\left(\frac{\tau_{\lambda_1}}{\tau_{\lambda_2}}\right)}{\ln\left(\frac{\lambda_1}{\lambda_2}\right)} \tag{13}$$

where α is the Ångström parameter, τ_a is the aerosol optical depth, and λ is the wavelength.

Atmospheric light extinction studies can be refined, to investigate the details of the spectral variation of this phenomenon, both inside the visible spectrum and outside. It is possible to obtain the dimensional distribution of the particles suspended in the atmosphere.

Measurements made by the solar photometer are transmitted directly to NASA via the internet. The scientific community can access this data from NASA servers for research and monitoring purposes. Data from the AERONET network is available online at http://aeronet.gsfc.nasa.gov/. AERONET data are corrected and processed at different levels of accuracy from 1 to 2, and more recently, at level 3.

3. Analysis of aerosol properties from the AERONET Eforie Nord station

3.1. Eforie Nord AERONET station

The AERONET sun-photometer (#397) – from Eforie Nord AERONET station – is placed on the roof of a building very close to the Black Sea's shore, at Dobrogea Seismological Observatory (Fig.3). This Observatory is located at the city Eforie Nord, in Dobrogea, on the Black Sea coast.

The station is 1 km away from the seaside (latitude: 44.075° N, longitude: 28.632° E, elevation: 40 meters). It is not influenced by industrial activities and intense traffic [15].

According to *climatological* data, Dobrogea is the warmest and the driest region of Romania.

Summer (early June to mid-September) is warm, dry and sunny with a July and August average of 23^{o} C.

The beginning of summer brings plenty of precipitation, but by early July the weather becomes settled and dry.

Most summer days see a gentle breeze refreshing the daytime temperatures. Nights are warm and somewhat muggy because of the heat stored by the sea.

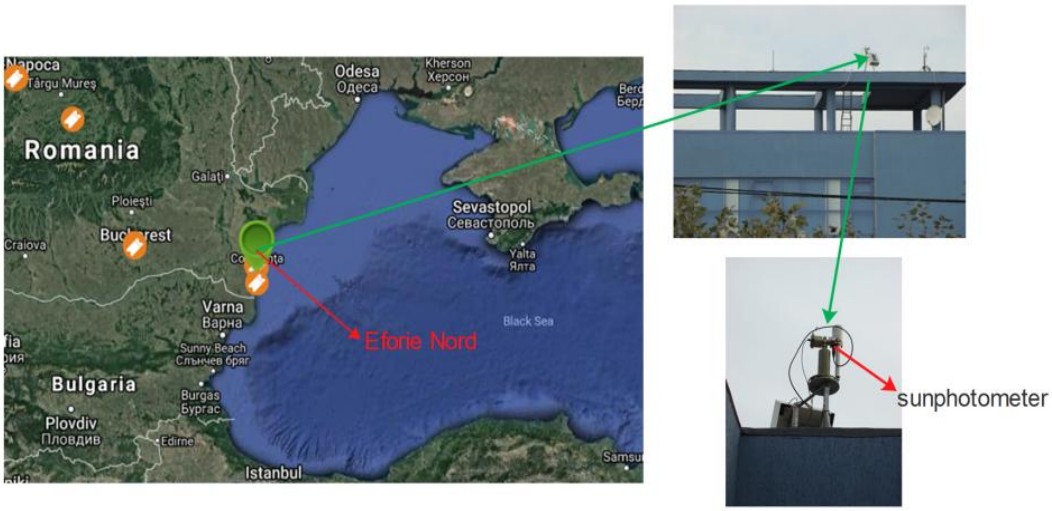

Fig. 3. Romanian Black Sea coast and the Eforie Nord AERONET site;
arrows indicate the position of the CIMEL sun photometer on the measurements platform
(Adapted from Google Earth and AERONET [15]).

Autumn starts in mid or late September with warm and sunny days.

September can be warmer than June, owing to the heat accumulated by the Black Sea.

The first frost occurs on average in mid-November [39].

The sun photometer data used in this study have been obtained by Cimel CE -318 instruments.

It is part of the AERONET global network [9] and Romanian network. Sun photometer measures the attenuation (every 15 min) in a 1.2 degree field of view, at eight solar spectral bands (340, 380, 440, 500, 670, 870, 940 and 1020 nm).

The solar extinction measurements are used to calculate for each wavelength the aerosol optical depth with an accuracy of about 0.01–0.02 AOD units [36].

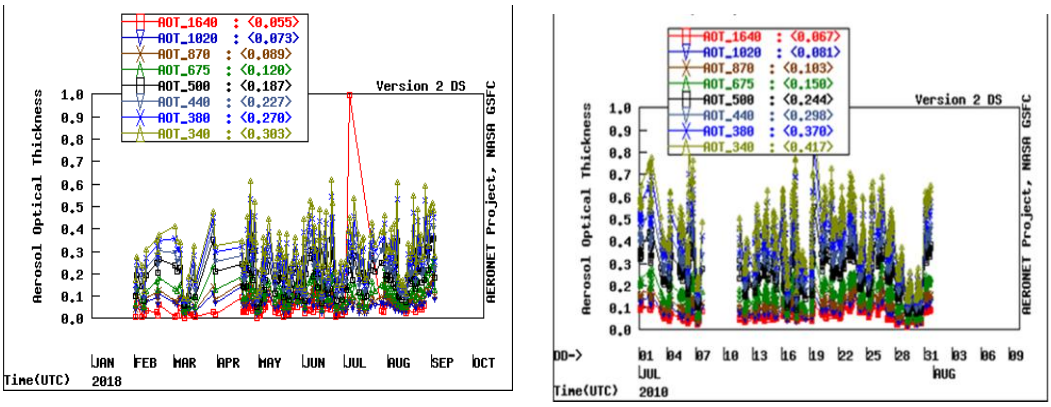

Fig. 4. AOD Level 2 data from year of 2010 and for month July 2010 Sun photometer acquires aerosol data only during daylight and in clear sky conditions.
In this study the cloud-screened monthly mean Level 2 data are used.

Figure 4 shows the Aerosol Optical Thickness (other name for AOD) for the 8 wavelengths of the sun-photometer. These charts are available on the Eforie Nord AERONET website (http://aeronet.gsfc.nasa.gov/).

3.2. Temporal variations of AOD and of the other optical parameters

Due to variations in sources and sinks, different aerosol components are associated with different geographical areas, and the residence time in the troposphere is relatively short (about 1 week). The vertical distribution of aerosol varies substantially, because it is determined by intrusion at height and the variety of atmospheric processes.

The AOD at 500nm is used to analyze its temporal variation. That is because the solar irradiance is most intense in the green/yellow part of the spectrum around 500 nm. The temporal variations of the columnar AOD are plotted in Fig.5 for 2010-2012 and 2015-2017 periods. These two periods were chosen to compare the aerosol properties under different meteorological conditions, because the frequency of severe weather events increased in the last years, especially in the south eastern part of Romania [40].

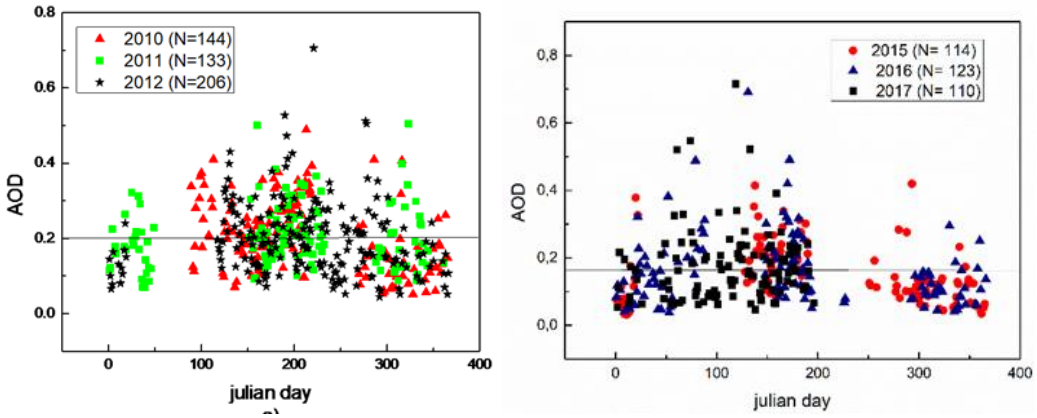

Fig. 5. The daily AOD values during 2010-2012 years (left chart [15]), and during 2015-2017 (right chart).

The small number of AOD (500) values in the second period, especially in 2017, should be noted.

The AOD(500) daily values during the 2010-2012 period vary between 0.04 to 0.50, with the mean value of 0.20±0.09. The AOD(500) values in 2015-2017 vary between 0.03 to 0.70, with the mean value of 0.11±0.02. In the summers of the 2010-2012 period, the average value of AOD was 0.218 ±0.082, bigger than the average value of 0.176 ± 0.042 for the summers of the 2015-2017 period. The highest values of AOD were recorded during summer and autumn days, and the lowest during winter.

Theoretically, the decrease of the AOD (presumably mainly anthropogenic aerosols) should coincide with the implementation of air quality legislation to reduce the emissions of pollutants, leading to an improvement in air quality. The decreasing numbers (N) of AOD values from the second period are particularly related to meteorological factors, which affect the size distribution of aerosols, and consequently, their properties. The relative humidity and the wind speed in the atmospheric boundary layer are both critical factors affecting the aerosols' characteristics. Furthermore, the increase in the number of days with nebulosity in the second period explains the low number of the AOD values [40]. The increase of the calibration period due to bad weather is added for the year 2017.

The wavelength-dependence of optical depth is usually represented by the Ångström parameter (α), an index of small particles and low values representative of large particles (Fig.6). The α parameter characterizes the spectral features of aerosols and it is mainly related to the size of the particles [41]. The α parameter is computed from AOD spectral values at two wavelengths, where absorption is negligible. In this case the two wavelengths are 440 and 870

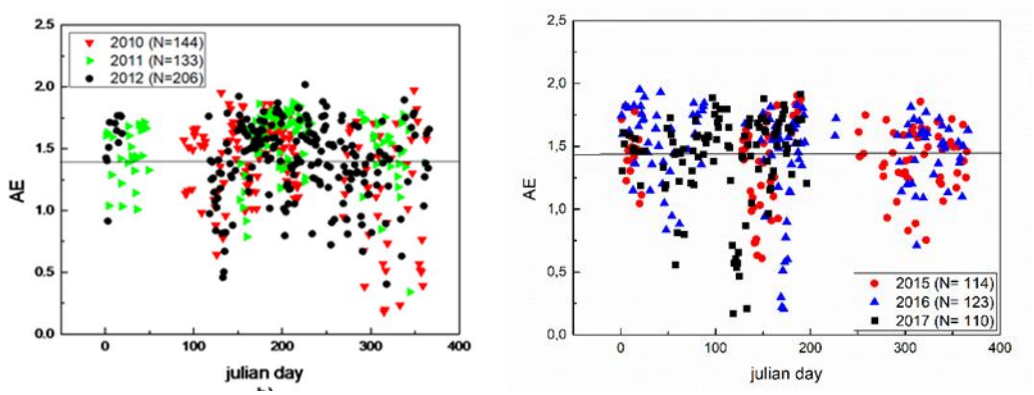

Fig. 6. The daily AE (440-870) values during 2010-2012 years (left chart[15], and during 2015-2017 (right chart).

The range of Ångström exponent daily values is 0.18 to 2.02, with the mean value of 1.42±0.33 during the 2010-2012 period.

During the period 2015-2017, daily AE values vary between 0.15 and 1.90. The mean values for the year 2011 and 2012, respectively, are 1.56±0.31 and 1.62±0.23, in the summer season [42].

It can be noted that the highest AE values (which means aerosols in fine mode) were recorded during summer and the lowest during autumn and winter.

The AE daily values reflect the persistent presence of fine aerosols during both analyzed periods.

Sporadically, coarse particles were noted during a few days in the spring, autumn and winter.

Size is one of the most important and commonly used aerosol classifications. Investigating whether fine or coarse modes are dominant provides important information on atmospheric air pollution. In this context, cases where the fine mode dominates the coarse mode can be associated with pollution episodes.

A fine mode fraction (FMF) is defined as the ratio of the AOD of the fine particles to the total AOD, which is used to represent the contribution of fine particles.

Fig.7 shows the daily FMF values during the two periods examined in this study. It can be noted that during these two periods, the FMF values for each year were over 0.6.

From the AERONET sun-photometer measurements, the aerosol types are classified on the basis of dominant size mode and radiation absorptivity.

The former is determined by the fine-mode fraction (FMF) and the latter by the single-scattering albedo (SSA) [43].

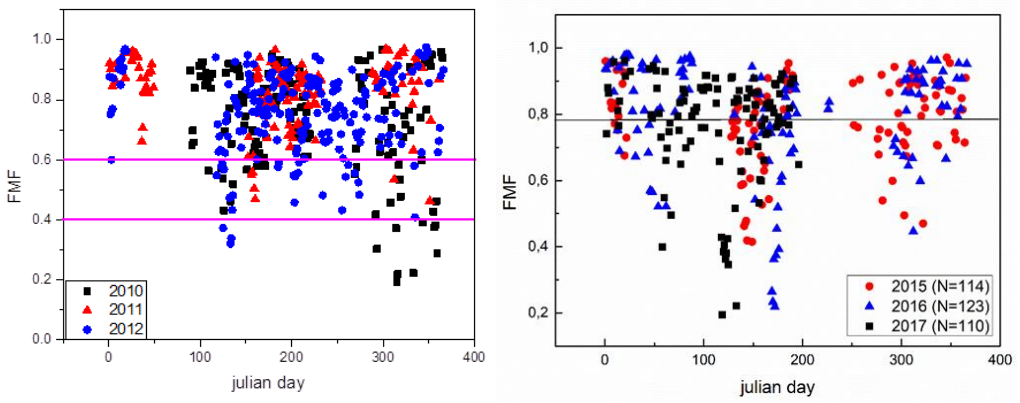

Fig. 7. The daily FMF values during 2010-2012 years (left chart) and during 2015-2017 (right chart).

Therefore, the simultaneous analysis of FMF and SSA discerns between aerosol types.

The direct effects of aerosols over land and at the bottom of the atmosphere are strongly dependent upon the aerosol single-scattering albedo (SSA). The SSA is a function of the size of particles, the state of the mixture, the wavelength, and the relative humidity.

Therefore, a characterization of aerosol absorption or SSA is complicated by instrumental errors and modeling inadequacies, as Dubovik *et al*. have shown (2001) [44].

The daily SSA values presented in Fig.8 are larger than 0.95 during the two periods. Due to SSA values and FMF values larger than 0.6, one can conclude that sea salt is the dominant aerosol. Sea salt is a non-absorbing aerosol, as Lee *et al*. (2010) have shown [43].

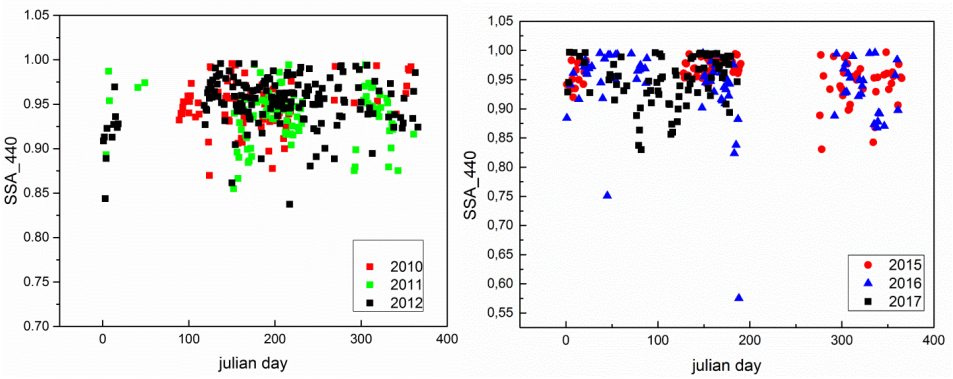

Fig. 8. The daily SSA values during 2010-2012 years (left chart) and during 2015-2017 (right chart).

The theoretical uncertainty of the AERONET retrieval of SSA is 0.03 for AOD greater than 0.3 [45]. The local assessment of both the aerosol absorption and SSA is important in regard to the quantification of the aerosol regional radiative forcing.

The results regarding the values of the aerosol optical parameters for the representative winter and summer months (Table 2) sustain the daily values presented so far for the two examined periods.

Tabel 2. Aerosol optical parameter values for the representative winter and summer months

Optical param. / Month	January 2010-2012	January 2015-2017	July 2010-2012	July 2015-2017
AOD	0.16±0.08	0.10±0.07	0.24±0.06	0.20±0.07
AE	1.49±0.27	1.53±0.21	1.54±0.31	1.54±0.23
FMF	0.89±0.08	0.87±0.09	0.79±0.11	0.84±0.08
SSA	0.92±0.04	0.96±0.03	0.95±0.02	0.92±0.11

3.3. Atmospheric turbidity at Eforie Nord AERONET station

The processes involved in atmospheric aerosol affect the air quality and its clarity, and cause air turbulence, especially in the lower troposphere. *Turbidity* is the physical parameter that shows how clean the atmospheric air is. It is a parameter of fundamental importance in air quality studies and climate changes. Therefore, atmospheric turbidity measurement is one of the most important data that can assess our planet's anthropogenic impact. The principles of solar photometry can be used as an important part of these measurements. There are several ways in the relevant scientific literature to define atmospheric turbidity. These are useful to interpret experimental data and to establish a common language in air quality analysis.

The spectrum of optical depth (AOD), τ_λ, is also called turbidity in studies dedicated to solar photometry. It can be noted, however, that this name is somewhat improper because the common meaning of the turbidity concept is that of measuring the degree of clarity of the atmosphere. However, the magnitude could be a measure of the air quality only for the wavelength λ. Further to this, all components of the atmospheric environment contribute to turbidity, including the molecules of gases that make up the atmosphere. This is despite the fact that turbidity only refers to the presence of suspended solids and liquids in the atmosphere.

The dependence of τ_λ on the wavelength of incident radiation is ultimately quite complicated, due to the diversity of atmospheric components.

However, for speedy practical evaluation purposes, an approximate expression called the *Ångstrom turbidity* equation [46] is used. This has fairly wide spectral limits, in which the wavelength dependence is reduced to inversed proportionality with a wavelength power:

$$\tau_\lambda = \beta \lambda^{-\alpha} \tag{14}$$

where β is the so-called *turbidity coefficient* (a dimensionless coefficient embedding the amount of aerosols in the atmosphere), and α is the *Ångström exponent* (AE) which is representative of the aerosol size distribution Relationship (14) clearly shows that the attenuation of radiation at any frequency decreases with the wavelength.

In general, the dependence of the optical depth on the wavelength is defined by the relationship of Eqs. 13. The advantage of the approximate relationship (14) is that the Ångström exponent (AE) can be determined by measuring the optical depth at only two different wavelengths, λ_1 and λ_2, and by calculating the ratio of the obtained values to simplify the turbidity coefficient (Eq. 13).

The usual values of turbidity vary from 0 to 0.5. The turbidity is considered within the following ranges: low, for values below 0.1; moderate, when it ranges between 0.1 and 0.3; and high, for values greater than 0.3 [47].

The values of the Ångström exponent AE (440-870) and AOD (500) were derived from the AERONET data, used in Section 3.2 above, to determine turbidity.

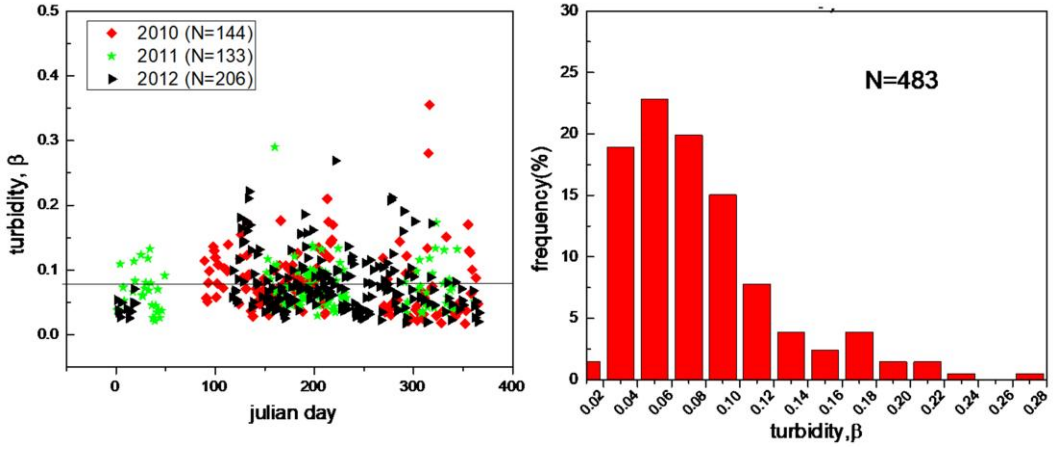

Fig. 9. Angstrom turbidity daily values (a) and relative frequency (b) during 2010-2012 period [15].

Daily Ångström turbidity coefficient was computed from Eq. (14). This study was carried out during the three years of the period 2010-2012.

The daily values of turbidity for the entire period 2010-2012 ranged from 0.02 to 0.30, with a mean value of 0.08±0.04 (Fig.9a). 78% of these turbidity values are lower than 0.1, whereas 22% belong to the interval 0.1-0.3 (Fig.9b). These values correspond to low and moderate turbidity in the atmosphere. The annual average values of turbidity show very little variations during the period of the study [15]: 0.08±0.05 (2010), 0.07±0.04 (2011) and 0.08±0.05 (2012). Thus, the values of the aerosol climatological parameters show a low turbidity for the Black Sea coast.

The turbidity is related to the columnar aerosol amount. As such, the results regarding the charging of the atmosphere with both natural and anthropic aerosol are found in the turbidity values. Additionally, it should be noted that the air quality in the atmosphere of the Black Sea Coast depends also on air circulation and meteorological conditions [15].

Conclusions

The observations from Eforie Nord AERONET site suggest a decreasing trend for the AOD (500) from mean values of (0.20±0.09) registered during 2010–2012 to mean values of (0.11±0.02) during 2015-2017. For the latter period, this decrease was also influenced by meteorological conditions. One can therefore conclude that the meteorological parameter associated with the air mass need to be considered in studies of optical properties of aerosols.

The seasonal behavior of the AOD exhibits a pattern with two maximal values, one in the spring, and a second one in the autumn. The AE parameter reaches a maximum value during summer (1.50) and its minimum during autumn (1.29). Its lowest values were registered in winter. These values indicate the predominant presence of small quantities of fine aerosols in the Black Sea coast's atmosphere.

The turbidity's annual average values show very little variations during the 2010-2012 period. That is because the aerosol loading is reduced.

The simultaneous analysis of the SSA and FFM values allows us to conclude that the aerosol particles at Eforie Nord have a mixed composition, dominated by sea salt.

It is also important to emphasize that the results obtained for these two periods using sun-photometer measurements can be used to determine the aerosol radiative forcing on the Black Sea Coast, as well as in studies of air quality.

Acknowledgments

The author would like to thank B.N.Holben (NASA's Goddard Space Flight Center, Greenbelt, MA) and Philippe Goloub (Photons, France) for making the AERONET database publicly available.

CIMEL sun-photometer calibration was performed at LOA using the AERONET-EUROPE calibration center, supported by the European Union's Horizon 2020 research and innovation program under grant agreement No 654109.

My thanks also, to Luk Blarel, Thierry Podvin, Gael Dubois and Livio Belegante for their care for, and maintenance of the sun-photometer.

R E F E R E N C E S

[1] IPCC: Climate Change **2007** - The Physical Science Basis: Working Group I Contribution to the Fourth Assessment Report of the IPCC.

[2] IPCC: *Climate Change **2013:** The Physical Science Basis*, Cambridge, UK and NY, USA

[3] S. Twomey, J. Atmos. Sci. **34**, 1149– 1152 (**1977**).

[4] B. A. Albrecht, Science **245**, 1227– 1230 (**1989**).

[5] Rosenfeld, D., I.M.Lensky, *Bulletin of the American Meteorological Society, **79***(11), 2457-2476, **1998**.

[6] C.I. Davidson *et al*., Aerosol Sci. Technol. **39**, 737–749, **2005**.

[7] J. O. Anderson *et al*., J. Med. Toxicol. **8**, 166–175, **2012**.

[8] K.H. Kim *et al*., Environ. Int. **74**, 136–143, **2015**.

[9] B.N. Holben, *et al*., 1998: AERONET - A federated instrument network and data archive for aerosol characterization, Rem. Sens. Environ., **66**, 1-16.

[10] S. Stefan *et al*., Environ. Engineering and Management Jour. (**10** (1), 147-153, **2011a**.

[11] S. Stefan *et al*., Environ. Engineering and Management Jour., **10 (**1), 133-138, **2011b**.

[12] L Filip, S. Stefan, Jour. of Atmosph. and Solar-Terrestrial Physics **77**, 104-112, **2012**.

[13] C.Grigoras, S.Stefan, Analysis of aerosol characteristics over different sites using AERONET and MODIS data, Proceedings of OTEM Conference Timisoara, sept **2013**, pp. 35-40.

[14] M. Gothard, A. Nemuc, C. Radu, S. Dascalu, Rom. Rep. Phys**. 66**, 509-519 (**2014**).

[15] S. Voinea, S. Stefan, Jour. of Atmos. and Solar-Terrestrial Physics **182**, 67-78, **2019**.

[16] S. Stefan, D. Nicolae, M. Caian, S*ecretele Aerosolului Atmosferic sub Lumina Laserilor* Ed. Ars Docendi, Bucuresti, Romania, **2008**.

[17] J.A. Coakley *et al*., Science (New York, N.Y.), **237**, 1020-1022, **1987**.

[18] Y.J. Kaufman, T. Nakajima, Journal of Applied Meteorology, **32**, 729-744 **1993**.

[19] Y.J. Kaufman *et al*., Journal of Geophysical Research, **102**, 17051, **1997**.

[20] V. Ramanathan *et al*., Science, **294** (5549), 2119-2124, **2001**.

[21] J. Hansen *et al*., Geophysical Research, **102**, 6831, **1997**.

[22] J. Seinfeld, S. Pandis, *Atmospheric Chemistry and Physics* - From Air Pollution to Climate Change (2nd Edition), John Wiley & Sons, **1998**.

[23] S. Stefan, *Physical Atmospheric Aerosol*, All Publishing, **1998**.

[24 M.Kulmala *et al*., Atmospheric Chemistry and Physics, 11, 10791-10801, **2011**.

[25] N.T. O'Neill *et al*., J. Geophys. Res. **106**, pp. 9787-9806, **2001**.

[26] N.T. O'Neill *et al*., J. Geophys. Res. **108(D17**), 4559, **2003**.

[27] J.W. Fitzgerald, J. Atmos. Sci., **35**, 1521, **1978**.

[28] J. Lee *et al*., Atmospheric Environment **44** (**2010**) 3110e3117

[29] I.I. Popescu, E.I. Toader, *Optica*, Ed, Stiintifica si anciclopedica, Bucuresti, **1989**.

[30] G. Mie., Beiträge zur Optik Trüber Medien, Speziell Kolloidaler Metallösungen, Annalen der Physik 25, 25-445, **1908**.

[31] J. P Buis *et al*., 1998). AERONET — A Federated Instrument Network and Data Archive for Aerosol Characterization. 4257.

[32] G. E. Shaw, *Sun Photometry.* Bulletin of the American Meteorological Society, **64**, 4-10, **1983**.

[33] D.M. Giles, Aerosol Robotic Network (AERONET) Homepage, **2014**.

[34] T. Nakajima *et al*., Applied Optics *35*(15), pp. 2672-2686, **1996**.

[35] O. Dubovik, M. D. King, J. Geophys. Res. **105**, pp. 20673-20696 (**2000**).

[36] T.F Eck, *et al*., J. Geophys. Res., **104**, 31 333-31 350, **1999**.

[37]B. Schmid *et al*., Appl. Opt. **40,** 1886-1896 (**2001**).

[38] A. Smirnov *et al*., Atmos. Meas. Tech. 4, 583–597, **2011**.

[39] I. Sandu, V.I. Pescaru, I. Poiana, A. Geicu, I. Candea, D. Tastea, *Clima Romaniei*, Academy Publ. House, Bucharest, Romania, **2008**.

[40] Z.Sipos, Manta D.R., Bulletin of Romanian Meteorology Society Anul IV no.1 (in Romanian Language), in http://smr.meteorolmania.ro

[41] J. Heintzenberg *et al*., Tellus, **52B**, 1104–1122, **2000**.

[42] C. Grigoras, *Contributii la studiul interactiei aerosol-nor (*PhD thesis), **2016**.

[43] J. Lee *et al*., Atmospheric Environment **44** 3110e3117, **2010**.

[44] O.Dubovik, King, M. D., J. Geophys. Res. **105,** 20673–20696, **2000**.

[45] O.Dubovik *et al*., J. Atmos. Sci. **59**, 590–608 **2002**.

[46] A. Ångström, On the atmospheric transmission of Sun radiation and on dust in the air. Geographical Annals **11,** 156–166.

[47] V. Hansen, Arch. Meteorol. Geophys. Bioklimatol., B **22**, 301–308, **1974**.